Biochemical and Biophysical Research Communications 394 (2010) 222–227

Contents lists available at ScienceDirect

Biochemical and Biophysical Research Communications

journal homepage: www.elsevier.com/locate/ybbrc

# A serine point mutation in the adenosine $A_{2A}R$ C-terminal tail reduces receptor heteromerization and allosteric modulation of the dopamine $D_2R$

Dasiel O. Borroto-Escuela [a,*], Daniel Marcellino [a], Manuel Narvaez [b], Marc Flajolet [c], Nathaniel Heintz [c], Luigi Agnati [d], Francisco Ciruela [e], Kjell Fuxe [a]

[a] Department of Neuroscience, Karolinska Institutet, Stockholm, Sweden
[b] Department of Physiology, School of Medicine, University of Málaga, Spain
[c] Laboratory of Molecular and Cellular Neuroscience, The Rockefeller University, NY, USA
[d] Department of Biochemical Sciences, University of Modena and IRCCS Lido, Venice, Italy
[e] Unitat de Farmacologia, Departament Patologia i Terapèutica Experimental, Facultat de Medicina, IDIBELL-Universitat de Barcelona, Barcelona, Spain

ARTICLE INFO

*Article history:*
Received 24 February 2010
Available online 1 March 2010

*Keywords:*
Dopamine $D_2$ receptor
Adenosine $A_2$ receptor
Heteromerization
G protein coupled receptors
Allosteric modulation
Protein–protein interaction

ABSTRACT

Evidence exists that the adenosine receptor $A_{2A}R$ and the dopamine receptor $D_2R$ form constitutive heteromers in living cells. Mass spectrometry and pull-down data showed that an arginine-rich domain of the $D_2R$ third intracellular loop binds via electrostatic interactions to a specific motif of the $A_{2A}R$ C-terminal tail. It has been indicated that the phosphorylated serine 374 might represent an important residue in this motif. In the present study, it was found that a point mutation of serine 374 to alanine reduced the $A_{2A}R$ ability to interact with $D_2R$. Also, this point mutation abolished the $A_{2A}R$-mediated inhibition of both the $D_2R$ high affinity agonist binding and signaling. These results point to a key role of serine 374 in the $A_{2A}R$–$D_2R$ interface. All together these results indicate that by targeting $A_{2A}R$ serine 374 it will be possible to allosterically modulate $A_{2A}R$–$D_2R$ function, thus representing a new approach for therapeutically modulate $D_2R$ function.



## 1. Introduction

Early behavioral observations with methylxanthines suggested the existence of antagonistic adenosine–dopamine interactions in the brain [1]. Later on, in the 1990s, indications were obtained that antagonistic intramembrane striatal adenosine $A_{2A}$ receptor ($A_{2A}R$) and dopamine $D_2$ receptor ($D_2R$) interactions were involved in mediating the enhancement due to L-DOPA and $D_2R$ agonist actions on movements [2,3]. Thus, the $A_{2A}R$ agonist CGS21680 reduced the affinity of the $D_2R$ agonist binding sites, especially those of high affinity in striatal membranes [2]. In 2002–2003, evidence was obtained using conventional biochemical techniques as well as bioluminescent and fluorescent techniques that $A_{2A}R$ and $D_2R$ can form constitutive heteromers in living cells, further supporting their existence in the brain [4,5]. Therefore, it was proposed that this antagonistic $A_{2A}R$–$D_2R$ interaction represented an allosteric mechanism by which $A_{2A}R$–$D_2R$ heteromers allowed proper neurotransmitter integration, especially in the striatum [6,7].

Electrostatic interactions between $D_2R$ and $A_{2A}R$ were discovered by mass spectrometry analysis and confirmed by biochemical pull-down assays. The regions involved are the N-terminal part of the intracellular loop 3 (IL3) of the short ($D_{2S}R$) and long ($D_{2L}R$) form of the $D_2R$ and the C-terminal domain of the $A_{2A}R$ receptor [8]. Specifically positively charged arginine-rich motif in the N-terminal part of $D_{2L}R$–IL3 interacted with two different negatively charged motif from the C-terminal part of the $A_{2A}R$, containing two adjacent aspartic residues or the phosphorylated serine residue (388-HELKGVCPEPPGLDDPLAQDGAVGS-412 and 370-SAQEpSQGNT-378), forming electrostatic bonds of covalent-like strength. The arginine–phosphate bond appeared to have a higher stability [9]. Serine 374 is also evolutionary conserved (see Supplementary Fig. 1).

Because charges seem to play a major role in this phenomenon and because phosphorylation sites can easily be regulated, we choose to focus our studies on putative phosphorylation sites. Therefore, in the present study we have tested the role of the $A_{2A}R$ serine 374 in the $A_{2A}R$–$D_{2L}R$ interface. It was found that while a point mutation of serine 374 to alanine in the $A_{2A}R$ C-terminal tail did not abolish the ability of $A_{2A}R$ and $D_{2L}R$ to co-immunoprecipitate, it significantly decreased the capacity of these receptors to heteromerize as demonstrated by means of FRET/BRET experiments. Interestingly, the mutation of this serine precluded the $A_{2A}R$-mediated allosteric modulation of $D_{2L}R$ as shown by means

* Corresponding author. Address: Department of Neuroscience, Karolinska Institutet, Retzius väg 8, 17177 Stockholm, Sweden. Fax: +46 8 315721.
*E-mail addresses:* Dasiel.Borroto-Escuela@ki.se, dasmel@gmail.com (D.O. Borroto-Escuela), Daniel.Marcellino@ki.se (D. Marcellino), mnarvaez@uma.es (M. Narvaez), flajolm@rockefeller.edu (M. Flajolet), luigiagnati@tin.it (L. Agnati), fciruela@ub.edu (F. Ciruela), Kjell.Fuxe@ki.se (K. Fuxe).

0006-291X/$ - see front matter © 2010 Elsevier Inc. All rights reserved.
doi:10.1016/j.bbrc.2010.02.168

of receptor competition binding experiments and receptor signaling approaches. Therefore the results indicated that the $A_{2A}R$ serine 374 plays a major role in the allosteric mechanism of the receptor interface mediating the inhibition of $D_2R$ recognition and signaling upon $A_{2A}R$ activation.

## 2. Materials and methods

### 2.1. Plasmid constructs

The cDNA encoding human $A_{2A}R$ cloned in pEYFP-N1 (Clontech, Germany) [10] was used as a template to mutate the serine 374 to alanine by means of the QuickChange™ site-directed mutagenesis kit (Stratagene, The Netherlands) following the manufacturer's protocol. On the other hand, the cDNA encoding the $D_{2L}R$ without its stop codon was subcloned in $pGFP^2$-N1 (Perkin-Elmer, Spain) and p*R*luc-N3 (Packard Bioscience, Spain) [10].

### 2.2. Cell culture, transfection and confocal microscopy

HEK293T cells (American Type Culture Collection, USA) were grown in Dulbecco's modified Eagle's medium supplemented with 2 mM L-glutamine, 100 U/ml penicillin/streptomycin, and 10% (v/v) fetal bovine serum (FBS) at 37 °C and in an atmosphere of 5% $CO_2$. For transfection, cells were plated in 6-well dishes at a concentration of $1 \times 10^6$ cells/well or in 75 $cm^2$ flasks and cultured overnight before transfection. Cells were transiently transfected either using linear PolyEthylenImine reagent (PEI) (Polysciences Inc., USA) or TransFectin (Bio-Rad, USA). Transiently transfected HEK293T cells were fixed in 4% paraformaldehyde for 10 min, washed with PBS containing 20 mM glycine and mounted with Vectashield immunofluorescence medium (Vector Laboratories, UK). Microscope observations were performed with a Leica TCS-SL confocal microscope (Leica, USA).

### 2.3. Co-immunoprecipitation and immunoblotting

For immunoprecipitation, HEK293T cells were harvested at 48 h after transfection and membrane solubilized in ice-cold radio immunoprecipitation assay (RIPA) buffer (50 mM Tris–HCl, pH 7.4, 100 mM NaCl, 1% Triton X-100, 0.5% sodium deoxycholate, 0.2% SDS and 1 mM EDTA) for 30 min on ice. The solubilized preparation was then centrifuged at 10,000*g* for 30 min. The supernatant (1 mg/ml) was processed for immunoprecipitation as previously described [10]. Then, proteins were transferred to PVDF membranes and immunoblotted with a mouse anti-$A_{2A}R$ monoclonal antibody (clone 7F6-G5-A2; 1:1000; Upstate, USA) or mouse anti-GFP monoclonal antibody (Sigma–Aldrich, Germany) and then a horseradish-peroxidase (HRP)-conjugated goat anti-mouse antibody (1:30,000; Pierce, USA). The immunoreactive bands were developed using a chemiluminescent detection kit [11].

### 2.4. Radioligand binding assay

Competition experiments of dopamine (0.3 nM to 3 mM) versus the $D_2$-like receptor antagonist [$^3$H]-Raclopride (~2 nM; 82.8 Ci/mmol) were carried out by incubation for 90 min at 30 °C in incubation buffer (IB: 20 mM Tris, 100 mM NaCl, 7 mM $MgCl_2$, 1 mM EDTA, 1 mM DTT, pH 7.4) in the presence or absence of CGS21680 (100 nM) and the incubation was terminated by rapid filtration through GF/B filters using a Brandel cell harvester with three washings of 5 ml of ice-cold washing buffer (WB: 20 mM Tris–HCl, pH 7.4, 100 mM NaCl). Saturation experiments with the $A_{2A}R$ antagonist [$^3$H]-ZM241385 (27.4 Ci/mmol) were carried out using 8 concentrations (0.09–6 nM) by incubation for 90 min at 30 °C in IB and the incubation was terminated as mentioned above. Nonspecific binding was defined as the binding in the presence of the $A_{2A}R$ antagonist MSX-3 (5 μM).

### 2.5. FRET experiments

HEK293T cells were transiently transfected with plasmids encoding $D_{2L}R^{GFP2}$ (donor) and $A_{2A}R^{YFP}$ or $A_{2A}R$-S374A$^{YFP}$ (acceptor) proteins as indicated for each experiment. Cells were suspended in PBS (4% glucose) and transferred into 96-well microplates (40 μg protein/well). FRET signals were collected using 410/10 nm excitation and 530/10 nm emission filters with a POLARstar Optima plate-reader (BMG Labtech, Offenburg, Germany). Removal of acceptor bleed-through and correction of acceptor fluorescence intensity changes were carried out as previously described [12].

### 2.6. BRET$^1$ assay

Forty-eight hours after transfection, HEK293T cells transiently transfected with constant (1 μg) or increasing amounts (0.5–6 μg) of plasmids encoding for $D_{2L}R^{Rluc}$ and $A_{2A}R^{GFP2}$ or $A_{2A}R$-S374A$^{GFP2}$, respectively, were rapidly washed twice in PBS, detached, and resuspended in the same buffer. Cell suspensions (20 μg protein) were distributed in duplicate into the 96-well microplate black plates with a transparent bottom (Corning 3651) (Corning, Stockholm, Sweden) for fluorescence measurement or white plates with a white bottom (Corning 3600) for BRET determination. For BRET$^1$ measurement, h-coelenterazine substrate (Molecular Probes, Eugene, OR, USA) was added at a final concentration of 5 μM, and readings were performed 1 min after using the POLARstar Optima plate-reader that allows the sequential integration of the signals detected with two filter settings [485 nm (440–500 nm) and 530 nm (510–560 nm)]. The BRET$^1$ ratio is defined as previously described [4].

### 2.7. Luciferase reporter gene assay

We used a dual luciferase reporter assay to indirectly detect variations of cAMP levels or activation of MAPK pathway in transiently transfected cell lines treated with different compounds in a range of concentrations (typically 25 nM to 1 μM). For luciferase assays, 24 h before transfection, cells were seeded at a density of $1 \times 10^6$ cells/well in 6-well dishes and transfected with PEI. Cells were co-transfected with plasmids corresponding to three constructs as follows (per 6-well): 1 μg firefly luciferase-encoding experimental plasmid (pGL4-CRE-luc2p or pGL4-SRE-luc2p; Promega, Stockholm, Sweden), 1 μg of $D_{2L}R^{GFP2}$ plus $A_{2A}R^{YFP}$ or $D_{2L}R^{GFP2}$ plus $A_{2A}R$-S374A$^{YFP}$ expression vectors and 50 ng *Renilla* luciferase-encoding internal control plasmid (phRG-B; Promega). Approximately 36 h post-transfection, after the cells were treated for 4 h with appropriate ligands and harvested with passive lysis buffer (Promega), the luciferase activity of cell extracts was determined using a luciferase assay system according to the manufacturer's protocol in a POLARstar Optima plate-reader (BMG Labtech) using a 30-nm bandwidth excitation filter at 535 nm. Firefly luciferase was measured as firefly luciferase luminescence over a 15 s reaction period. The luciferase values were normalized against *Renilla* luciferase luminescence values. Transfection experiments were performed in quadruplicate and repeated at least three times.

### 2.8. Statistical analysis

The number of samples ($n$) in each experimental condition is indicated in figure legends. When two experimental conditions were compared, statistical analysis was performed using an unpaired $t$ test. Otherwise, statistical analysis was performed by

one-way analysis of variance (ANOVA) followed by Tukey's Multiple Comparison post-test. The *P* value 0.05 and lower was considered significant.

## 3. Results

### 3.1. Adenosine and dopamine receptor heteromerization

In order to study the postulated role of the $A_{2A}R$ serine 374 in the $A_{2A}R$–$D_{2L}R$ heteromerization this amino acid was mutated to alanine to prevent its phosphorylation and to test its ability to heterodimerize with $D_{2L}R$ [8]. By means of fluorescence detection we found that $A_{2A}R^{YFP}$ and $A_{2A}R$-S374A$^{YFP}$ were expressed at the plasma membrane (Fig. 1A and B) as the $D_{2L}R^{GFP2}$ (Fig. 1C). An in depth study of the subcellular localization of $A_{2A}R$-S374A$^{YFP}$ showed a more punctuated intracellular distribution compared to the $A_{2A}R^{YFP}$ that has a more reticular distribution (Fig. 1A and B). Interestingly, when $A_{2A}R^{YFP}$ and $A_{2A}R$-S374A$^{YFP}$ were co-expressed with $D_{2L}R^{GFP2}$ both adenosine receptor fusion proteins showed a high degree of co-distribution with the $D_{2L}R^{GFP2}$ (Fig. 1F and I). Thus, in the presence of $D_{2L}R^{GFP2}$ the $A_{2A}R$-S374A$^{YFP}$ plasma membrane location is maintained (Fig. 1G).

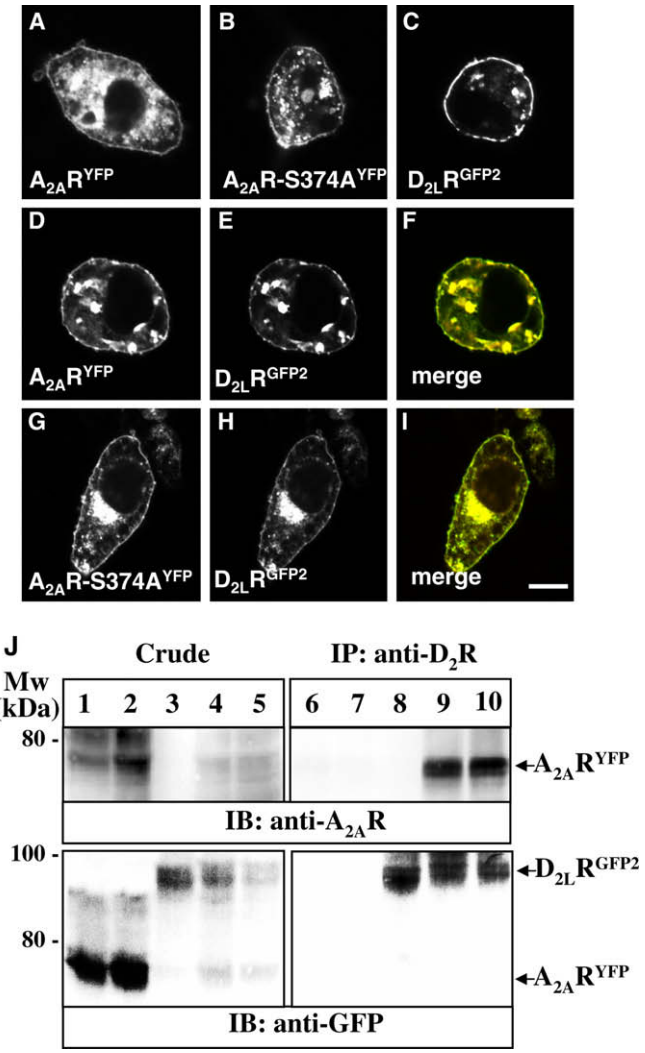


**Fig. 1.** $A_{2A}R$/$D_{2L}R$ co-localize and heterodimerize in HEK293T cells. (A–I) Co-localization (presence in the same micro-domain of the membrane) studies of adenosine $A_{2A}R$ and dopamine $D_{2L}R$ receptors. HEK293T transiently transfected with $A_{2A}R^{YFP}$ (A), $A_{2A}R$-S374A$^{YFP}$ (B), $D_{2L}R^{GFP2}$ (C), $A_{2A}R^{YFP}$ plus $D_{2L}R^{GFP2}$ (D, E, F) and $A_{2A}R$-S374A$^{YFP}$ plus $D_{2L}R^{GFP2}$ (G, H, I) were fixed and analyzed by confocal microscopy. Superimposition of images reveals a co-distribution of $A_{2A}R^{YFP}$–$D_{2L}R^{GFP2}$ and $A_{2A}R$-S374A$^{YFP}$–$D_{2L}R^{GFP2}$ (merge). Scale bar: 10 μm. (J) Co-immunoprecipitation studies of $A_{2A}R$ and $D_{2L}R$ receptors. HEK293T cells transiently expressing $A_{2A}R^{YFP}$ (lanes 1 and 6), $A_{2A}R$-S374A$^{YFP}$ (lanes 2 and 7), $D_{2L}R^{GFP2}$ (lanes 3 and 8), $A_{2A}R^{YFP}$ plus $D_{2L}R^{GFP2}$ (lanes 4 and 9) and $A_{2A}R$-S374A$^{YFP}$ plus $D_{2L}R^{GFP2}$ (lanes 5 and 10) were washed, solubilized and processed for immunoprecipitation using a rabbit anti-$D_2R$ antibody (2 μg/ml; IP: anti-$D_2R$). Solubilized membranes (Crude) and immunoprecipitates (IP) were analyzed by SDS–PAGE and immunoblotted.

Also, from extracts of HEK293T cells transiently transfected with $A_{2A}R^{YFP}$ plus $D_{2L}R^{GFP2}$, the rabbit anti-$D_2R$ antibody co-immunoprecipitated a protein of molecular weight ~75 kDa which corresponds to the $A_{2A}R^{YFP}$ (Fig. 1J, IP: anti-$D_2R$, lane 9). This protein band did not appear in singly transfected cells immunoprecipitated with the same antibody (Fig. 1J, IP: anti-$D_2R$, lanes 6, 7 and 8). Importantly, the anti-$D_2R$ antibody was able to co-immunoprecipitate the $A_{2A}R$-S374A$^{YFP}$ from cells doubly transfected with $A_{2A}R$-S374A$^{YFP}$ and $D_{2L}R^{GFP2}$ (Fig. 1J, IP: anti-$D_2R$, lane 10). Overall, these results suggested that the $A_{2A}R$ serine 374 mutation do not affect co-distribution and co-immunoprecipitation of $A_{2A}R$ and $D_{2L}R$.

Next, we studied the role of the $A_{2A}R$ serine 374 in the $A_{2A}R$–$D_{2L}R$ heteromerization by means of FRET and BRET experiments. FRET assay was performed on HEK293T cells co-expressing a constant amount of $D_{2L}R^{GFP2}$ and of the $A_{2A}R^{YFP}$ or of the $A_{2A}R$-S374A$^{YFP}$ mutant plasmids (donor:acceptor ratio 1:2 μg cDNA). As a positive control, we used the cell expressing a GFP$^2$-YFP tandem fusion protein (0.5 μg cDNA). Upon co-expression of the $D_{2L}R^{GFP2}$ and $A_{2A}R^{YFP}$ cDNA, a significantly higher FRET signal was observed compared to the FRET signal obtained from cells individually expressing each of the two receptors (Fig. 2A). However, cells co-expressing $D_{2L}R^{GFP2}$ and $A_{2A}R$-S374A$^{YFP}$ resulted in a significant 1.5-fold reduction in the FRET signal compared to the wild-type receptor (Fig. 2A).

In addition, a BRET saturation curve was constructed in HEK293T cells co-transfected with a constant amount of $D_{2L}R^{Rluc}$ construct while increasing the concentrations of the $A_{2A}R^{YFP}$ plasmid or the $A_{2A}R$-S374A$^{YFP}$ mutant plasmid. A positive BRET signal was obtained for the transfer of energy between $D_{2L}R^{Rluc}$ and $A_{2A}R^{YFP}$. The BRET signal as seen from the BRET[1] ratio increased as a hyperbolic function of the concentration of the $A_{2A}R^{YFP}$ fusion construct (Fig. 2B filled square). The pair $D_{2L}R^{Rluc}$ and $A_{2A}R$-S374A$^{YFP}$ led to a substantial reduction in the BRET signal versus the $D_{2L}R^{Rluc}$ and $A_{2A}R^{YFP}$ pair as seen from the marked reduction of the $BRET_{max}$ values (Fig. 2B filled circle). When $D_{2L}R^{Rluc}$ singly expressing cells and $A_{2A}R^{YFP}$ singly expressing cells were mixed no BRET signal was observed.

### 3.2. $D_{2L}R$ radioligand competition experiments: [$^3$H]-Raclopride versus DA

The results from the transiently $A_{2A}R^{YFP}$–$D_{2L}R^{GFP2}$ and $A_{2A}R$-S374A$^{YFP}$–$D_{2L}R^{GFP2}$ co-transfected HEK293T cells are shown in Fig. 3. The competition curves were characterized by the existence of two binding sites for dopamine, one with the dissociation constant in the high affinity state ($K_H$) and another with the dissociation constant ($K_L$) in the low affinity state. The $A_{2A}R$ agonist CGS21680 (100 nM) preferentially and significantly increased the $K_H$ value of the $D_{2L}R$ agonist binding site in the $D_{2L}R^{GFP2}$ construct after activation of the $A_{2A}R^{YFP}$ construct. In contrast, CGS21680 (100 nM) failed to alter the affinity of the $K_H$ value of the $D_{2L}R$ agonist binding site in the $D_{2L}R^{GFP2}$ construct after activation of the point mutated $A_{2A}R$-S374A$^{YFP}$ construct (Fig. 3B). The expression of $D_{2L}R^{GFP2}$ in the two types of cells was similar, 6 pmol/mg protein ($A_{2A}R^{YFP}$–$D_{2L}R^{GFP2}$) and 4 pmol/mg protein ($A_{2A}R$-S374A$^{YFP}$–$D_{2L}R^{GFP2}$).

### 3.3. Functional implications of S374A point mutation

A schematic diagram of the principle of the SRE-luciferase reporter assay under the control of the $A_{2A}R$–$D_{2L}R$ heteromer and

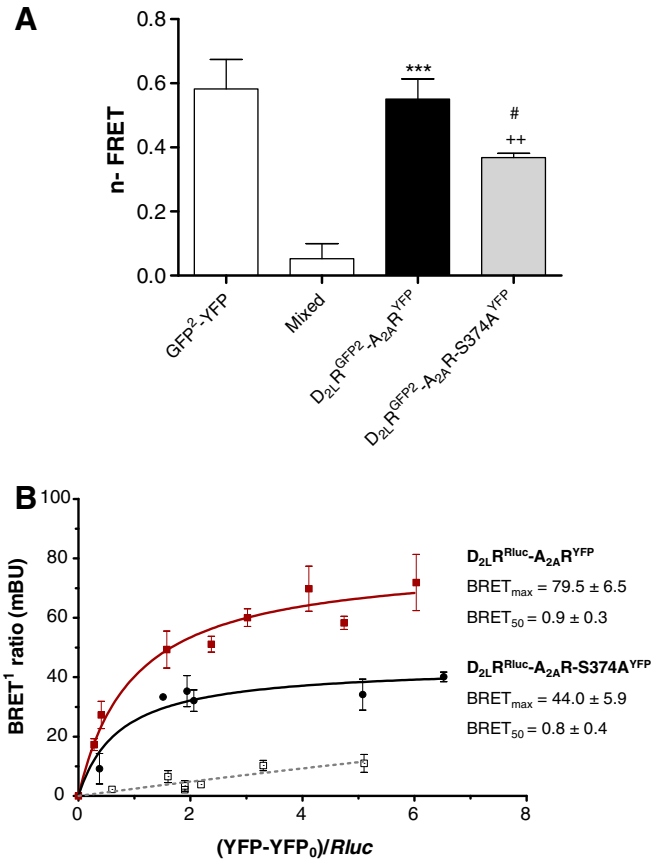


**Fig. 2.** FRET and BRET studies of $A_{2A}R$ and $D_{2L}R$ heteromerization in HEK293T cells. (A) FRET experiments. HEK293T cells were transiently transfected with 1 μg of plasmid encoding $D_{2L}R^{GFP2}$ (donor) and 2 μg of plasmid encoding either $A_{2A}R^{YFP}$ or $A_{2A}R$-S374A$^{YFP}$ (acceptor), or with 0.5 μg of the positive control plasmid GFP$^2$-YFP. Fluorescence readings were performed 48 h after transfection and the results are shown as the intensity of normalized FRET measurement. For negative controls, mixed populations of cells transfected solely with $D_{2L}R^{GFP2}$ or $A_{2A}R^{YFP}$ fusions were used (see also [4]). Data are expressed as the mean ± SEM of three independent experiments performed in triplicate. ***Significantly different compared to mixed ($P < 0.001$). $^{++}$Significantly different compared to mixed ($P < 0.01$). $^{\#}$Significantly different compared to $D_{2L}R^{GFP2}$–$A_{2A}R^{YFP}$ ($P < 0.05$). (B) BRET saturation curves for the $D_{2L}R$–$A_{2A}R$ hetero-oligomers ($D_{2L}R^{Rluc}$ + $A_{2A}R^{YFP}$, filled square) compared to $D_{2L}R$–$A_{2A}R$-S374A hetero-oligomers ($D_{2L}R^{Rluc}$ + $A_{2A}R$-S374A$^{YFP}$, filled circle) at increasing expression levels of the YFP tagged receptor. Cell individually expressing $D_{2L}R^{Rluc}$ were mixed prior exposition to h-coelenterazine with cells individually expressing $A_{2A}R^{YFP}$ as a negative control (square). Plotted on the *X*-axis is the fluorescence value obtained from the YFP, normalized with the luminescence value of $D_{2L}R$-Rluc expression 10 min after h-coelenterazine incubation. Mean ± SEM; $n = 8$ in triplicate.

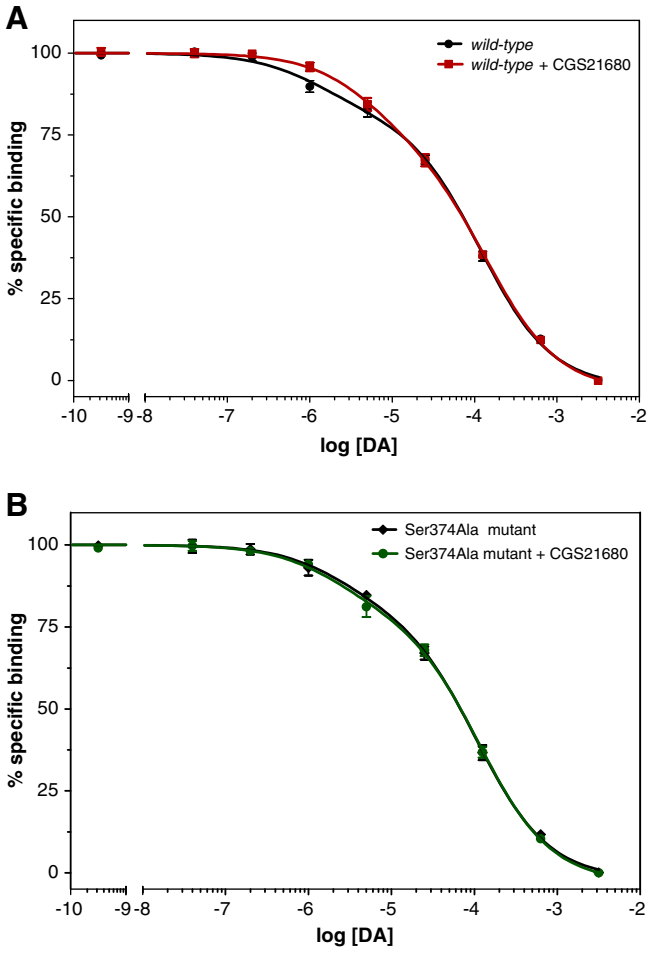


**Fig. 3.** The $A_{2A}R$ receptor agonist-mediated modulation of $D_{2L}R$ agonist binding. Competition experiments of the $D_2$-like receptor antagonist [$^3$H]-Raclopride (2 nM) versus increasing concentrations of dopamine in transiently co-transfected HEK293T cell membranes. (A) $D_{2L}R$ agonist competition experiments with dopamine (■) were performed in the absence (●) or the presence (■) of the $A_{2A}R$ agonist CGS21680 (200 nM) [log $K_i$ low = −4.44 ± 0.05 and −4.39 ± 0.01; log $K_i$ high = −6.28 ± 0.09 and −5.67 ± 0.07, respectively; (∗) $P < 0.05$]. (B) Competition experiments with dopamine upon cotransfection of the $A_{2A}R$-S374A$^{YFP}$ were performed in the absence (♦) or the presence (●) of the $A_{2A}R$ agonist CGS21680 (200 nM) [log $K_i$ low = −4.49 ± 0.08 and −4.43 ± 0.03; log $K_i$ high = −6.18 ± 0.25 and −6.17 ± 0.12, respectively]. Data are the means ± SEM from four separate experiments performed in duplicate.

Receptor Tyrosine Kinase (RTK) is shown in Fig. 4A. Direct and indirect interactions between $A_{2A}R$–$D_{2L}R$ heteromer and RTK, involving the beta–gamma subunits, modulate the activity of the Ras–Raf–MEK1–MAPK pathway to the SRE [13]. The antagonistic allosteric receptor–receptor interaction in the $A_{2A}R$–$D_{2L}R$ heteromer is indicated. The results from $A_{2A}R^{YFP}$–$D_{2L}R^{GFP2}$ and $A_{2A}$R-S374A$^{YFP}$–$D_{2L}R^{GFP2}$ co-transfected HEK293T cells are shown (Fig. 4B and C). In $A_{2A}R^{YFP}$–$D_{2L}R^{GFP2}$ transfected cells (Fig. 4B), the dopamine $D_2$ like agonist quinpirole (25 nM) markedly induced SRE which was blocked by the dopamine $D_2$ like antagonist raclopride and substantially reduced by the adenosine $A_{2A}$ agonist CGS21680 (50 nM). In $A_{2A}$R-S374A$^{YFP}$–$D_{2L}R^{GFP2}$ transfected cells (Fig. 4C), CGS21680 failed to reduce the quinpirole-induced SRE activation but were again fully counteracted by raclopride.

Furthermore, $A_{2A}R$ activation can, via the $G_s$-AC-PKA cascade (AC: adenylate cyclase) increase the phosphorylation of CREB leading to an increase of the CRE transcription. $A_{2A}R$ activation can also lead to an increased transcriptional activity by antagonizing the $D_{2L}R$-$G_{o/i}$-AC inhibition through a receptor–receptor interaction. In $A_{2A}R^{YFP}$–$D_{2L}R^{GFP2}$ transfected cells, the forskolin-induced increase of luciferase activity by a direct activation of AC is significantly reduced by quinpirole, an action which is fully counteracted by 50 nM of CGS21680 and by the $D_2R$ like antagonist raclopride (1 μM) (Supplementary Fig. 2B). CGS21680 (50 nM) alone does not affect the forskolin-induced increase of luciferase activity but the activity is $A_{2A}R$-dependent since the $A_{2A}R$ antagonist ZM241385 reduces the luciferase activity to a similar level as found after quinpirole. However, in $A_{2A}$R-S374A$^{YFP}$–$D_{2L}R^{GFP2}$ cells (Supplementary Fig. 2C) with the single point mutated $A_{2A}R$ it is no longer possible for CGS21680 (50 nM) to counteract the quinpirole induced reduction of luciferase activity, while raclopride (1 μM) is still able to counteract it. The forskolin stimulated luciferase activity remains dependent on $A_{2A}R$ activity, since the $A_{2A}R$ antagonist ZM241385 reduces it to the same degree as found in cells with $A_{2A}R^{YFP}$. In the absence of forskolin, the mutant $A_{2A}R$ and the wild-type $A_{2A}R$ receptors lead to the same level of CRE induction in response to CGS21680 (50 nM) (Supplementary

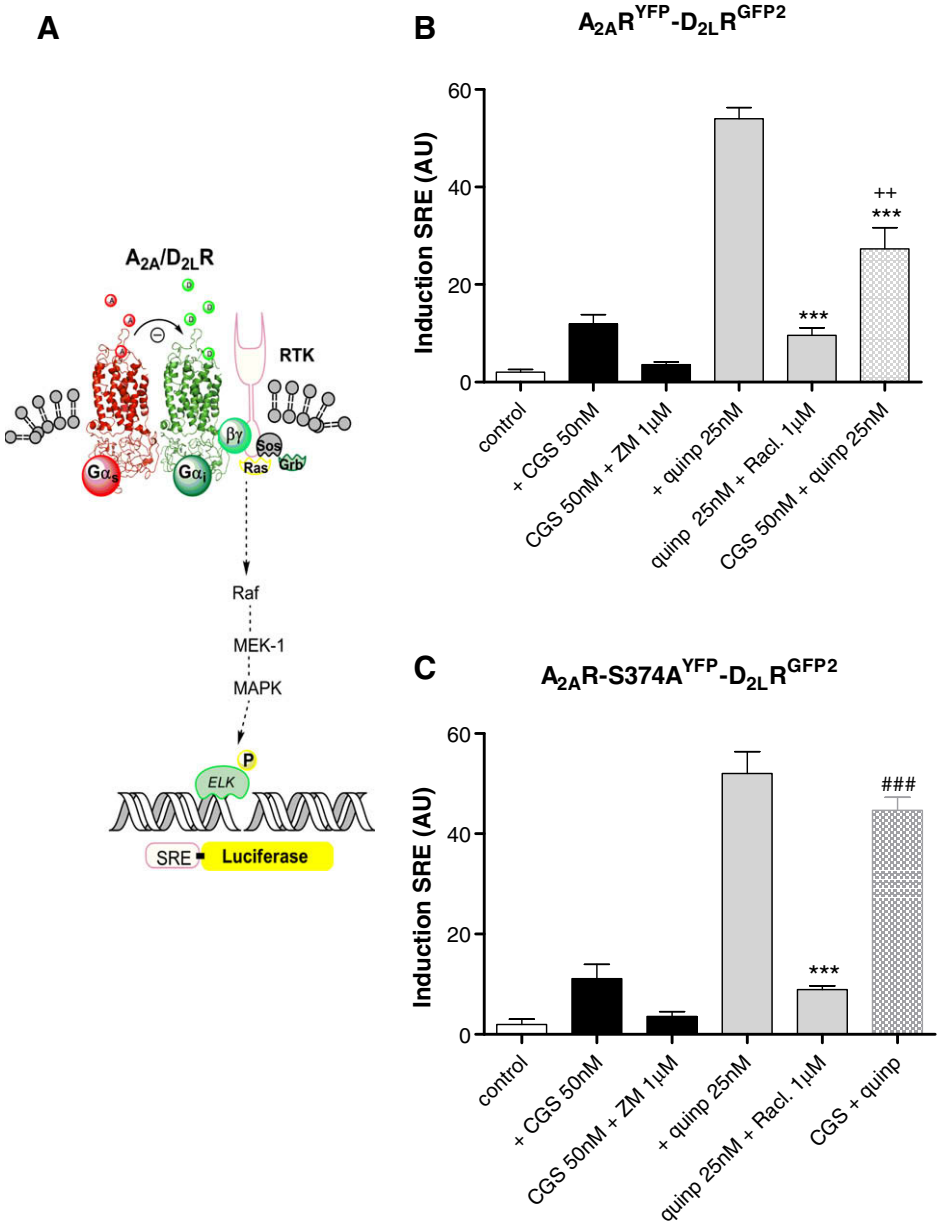


**Fig. 4.** SRE reporter assay response after $D_{2L}R$ and $A_{2A}R$ activation. (A) Schematic cross-talk signaling pathway of $A_{2A}R$ and $D_{2L}R$ receptor and the firefly luciferase gene regulated by the SRE response element. HEK293T cells were transiently co-transfected with 1 μg firefly luciferase-encoding experimental plasmid (pGL4-SRE-luc2p), 1 μg of both ($D_{2L}R^{GFP2}$ and $A_{2A}R^{YFP}$) (B) or ($D_{2L}R^{GFP2}$ and $A_{2A}R$-S374A$^{YFP}$) (C) expression vectors and 50 ng *Renilla* luciferase-encoding internal control plasmid (phRG-B). Thirty-six hours after transfection, cells were treated 4 h with agonist or antagonist (in presence of agonist). The data represent the means ± SEM of three independent experiments performed in triplicate. ***Significantly different compared to quinp 25 nM ($P < 0.001$). ++Significantly different compared to CGS 50 nM ($P < 0.01$). ###Significantly different compared to CGS 50 nM ($P < 0.001$). CGS, CGS21680 (50 nM); ZM, ZM241385 (1 μM); quinp, quinpirol (25 nM) and racl, raclopride (1 μM).

Fig. 3A and B). Furthermore, quinpirole reduced the $A_{2A}R$-mediated induction of CRE.

## 4. Discussion

The present findings demonstrate that the mutation of a single residue, the serine 374 mutated to alanine, in the C-terminal domain of the $A_{2A}R$ has an impact on the $D_{2L}R^{GFP2}$–$A_{2A}R^{YFP}$ heteromer. Indeed, this single point mutation reduces the FRET and BRET signals emitted by the $D_{2L}R$–$A_{2A}R$ heteromer. This mutation fully counteracts the ability of the activated $A_{2A}R^{YFP}$ to increase the $K_D$ value of the high affinity $D_{2L}R$ agonist binding sites and to counteract the ability of activated $A_{2A}R$ to inhibit $D_2R$ agonist mediated induction of SRE. Furthermore, it counteracts the $D_{2L}R$ agonist mediated reduction of forskolin-induced CRE transcription. These results therefore strongly indicate that the major role of the serine 374 is in mediating the allosteric receptor–receptor interactions since the BRET and FRET signals still exist although reduced. Importantly, the $A_{2A}R$-S374A$^{YFP}$ mutant receptor is correctly addressed to the plasma membrane and it co-localizes with the $D_{2L}R^{GFP2}$ receptor. It is also functionally coupled to downstream signaling pathways and its activation leads to efficient SRE/CRE activation.

The present observations therefore give further evidence that the serine in the C-terminal domain of the $A_{2A}R$ represents a hot spot in the part of the $A_{2A}R$–$D_{2L}R$ interface. It may be located between the negatively charged motif in the C-terminal domain of

the $A_{2A}R$ and the positively charged motif in the N-terminal part of the IL3 (arginine-rich domain) of the $D_{2L}R$ [4,8]. This serine has been predicted to be constitutively phosphorylated, thus increasing the negative charge of this domain and the columbic force that mediate this interaction [8,14]. This may be the reason why the point mutation has a dramatic impact on the total negative charge of this motif. The correct three dimensional structure of the $A_{2A}R$–$D_{2L}R$ complex apparently remains intact despite the mutation but the FRET signal is markedly reduced indicating that part of the $A_{2A}R$–$D_{2L}R$ interface is altered most likely due to failures in the electrostatic receptor–receptor interactions leading to a partial disengagement of the two fluorophores. It has been proposed that the arginine–phosphate electrostatic interaction represents a general mechanism in protein–protein interactions [14]. Thus, in our model, the molecular proximity was reduced by the alanine mutation and the remaining FRET/BRET signal observed might be due to receptor–receptor interaction involving other receptor regions such as transmembrane domains [15,16].

It is of substantial interest that the mutation of the phosphorylated serine in the $A_{2A}R$ disrupted the antagonistic allosteric $A_{2A}R$–$D_{2L}R$ receptor–receptor interactions both in terms of $D_{2L}R$ recognition and of $D_{2L}R$ signaling. Thus, allosteric communication between the $A_{2A}R$ and $D_{2L}R$ receptors requires the arginine–phosphate bond at least with regard to these fundamental functions of the $D_{2L}R$ receptor. However, it is important to notice that in contrast this mutant $A_{2A}R$ receptor can still signal as seen from its intact ability to cause an induction of SRE/CRE upon activation by an $A_{2A}R$ agonist. Also its signaling can be significantly reduced by the $D_{2L}R$ agonist quinpirole as is the signaling of the intact $A_{2A}R$ receptor. The physiological role of serine 374 on the $A_{2A}R$–$D_2R$ heterodimer is also implied by the high degree of conservation of serine 374 among heterologous species (Supplementary Fig. 1). It should also be considered that not only regulation of one serine but possibly two serines (S370 and S374) could be involved. We therefore hypothesize a novel function for the phospho residues of Class A GPCR C-terminal tails: the stabilization of heterodimers. For all these reasons, the $A_{2A}R$-S374A mutant receptor represents a novel and unique approach to further investigate the physiological relevance of $A_{2A}R$–$D_{2L}R$ heteromerization *in vivo* in the central nervous system.

In conclusion, it was found that a point mutation of serine 374 to alanine reduced the $A_{2A}R$ ability to interact with $D_2R$ and abolished the $A_{2A}R$-mediated inhibition of both the $D_2R$ high affinity agonist binding and signaling. These results point to a key role of serine 374 in the $A_{2A}R$–$D_2R$ interface, indicating that by targeting $A_{2A}R$ serine 374 it will be possible to allosterically modulate the $D_2R$ function of the $A_{2A}R$–$D_2R$ heteromers.

## Acknowledgments

This work was supported by grants from the Swedish Research Council (04X-715), Torsten and Ragnar Söderberg Foundation, Hjärnfonden and Marianne and Marcus Wallenberg Foundation to K.F. and SAF2008-01462 and Consolider-Ingenio CSD2008-00005 from Ministerio de Ciencia e Innovación to F.C. We thank Dr. Paul Greengard for his constructive suggestions.

## Appendix A. Supplementary data

Supplementary data associated with this article can be found, in the online version, at doi:10.1016/j.bbrc.2010.02.168.

## References

[1] K. Fuxe, U. Ungerstedt, Action of caffeine and theophyllamine on supersensitive dopamine receptors: considerable enhancement of receptor response to treatment with DOPA and dopamine receptor agonists, Med. Biol. 52 (1974) 48–54.
[2] S. Ferre, G. von Euler, B. Johansson, B.B. Fredholm, K. Fuxe, Stimulation of high-affinity adenosine A2 receptors decreases the affinity of dopamine D2 receptors in rat striatal membranes, Proc. Natl. Acad. Sci. USA 88 (1991) 7238–7241.
[3] K. Fuxe, S. Ferré, P. Snaprud, G. von Euler, B. Johansson, B.B. Fredholm, Antagonistic A2A/D2 receptor interaction in the striatum as a basis fro adenosine/dopamine interactions in the central nervous system, Drug Dev. Res. 28 (1993) 374–380.
[4] M. Canals, D. Marcellino, F. Fanelli, F. Ciruela, P. de Benedetti, S.R. Goldberg, K. Neve, K. Fuxe, L.F. Agnati, A.S. Woods, S. Ferre, C. Lluis, M. Bouvier, R. Franco, Adenosine A2A–dopamine D2 receptor–receptor heteromerization: qualitative and quantitative assessment by fluorescence and bioluminescence energy transfer, J. Biol. Chem. 278 (2003) 46741–46749.
[5] T. Kamiya, O. Saitoh, K. Yoshioka, H. Nakata, Oligomerization of adenosine A2A and dopamine D2 receptors in living cells, Biochem. Biophys. Res. Commun. 306 (2003) 544–549.
[6] L.F. Agnati, D. Guidolin, G. Leo, C. Carone, S. Genedani, K. Fuxe, Receptor–receptor interactions: a novel concept in brain integration, Prog. Neurobiol. 90 (2010) 157–175.
[7] K. Fuxe, D. Marcellino, A. Rivera, Z. Diaz-Cabiale, M. Filip, B. Gago, D.C. Roberts, U. Langel, S. Genedani, L. Ferraro, A. de la Calle, J. Narvaez, S. Tanganelli, A. Woods, L.F. Agnati, Receptor–receptor interactions within receptor mosaics. Impact on neuropsychopharmacology, Brain Res. Rev. 58 (2008) 415–452.
[8] F. Ciruela, J. Burgueno, V. Casado, M. Canals, D. Marcellino, S.R. Goldberg, M. Bader, K. Fuxe, L.F. Agnati, C. Lluis, R. Franco, S. Ferre, A.S. Woods, Combining mass spectrometry and pull-down techniques for the study of receptor heteromerization. Direct epitope–epitope electrostatic interactions between adenosine A2A and dopamine D2 receptors, Anal. Chem. 76 (2004) 5354–5363.
[9] S.N. Jackson, H.Y. Wang, A. Yergey, A.S. Woods, Phosphate stabilization of intermolecular interactions, J. Proteome Res. 5 (2006) 122–126.
[10] N. Cabello, J. Gandia, D.C. Bertarelli, M. Watanabe, C. Lluis, R. Franco, S. Ferre, R. Lujan, F. Ciruela, Metabotropic glutamate type 5, dopamine D2 and adenosine A2a receptors form higher-order oligomers in living cells, J. Neurochem. 109 (2009) 1497–1507.
[11] F. Ciruela, R.A. McIlhinney, Differential internalisation of mGluR1 splice variants in response to agonist and phorbol esters in permanently transfected BHK cells, FEBS Lett. 418 (1997) 83–86.
[12] D.O. Borroto-Escuela, M. Narvaez, D. Marcellino, C. Parrado, J.A. Narvaez, A.O. Tarakanov, L.F. Agnati, Z. Diaz-Cabiale, K. Fuxe, Galanin receptor-1 modulates 5-hydroxtryptamine-1A signaling via heterodimerization, Biochem. Biophys. Res. Commun. (2010), doi:10.1016/j.bbrc.2010.02.078.
[13] C. Wang, D.C. Buck, R. Yang, T.A. Macey, K.A. Neve, Dopamine D2 receptor stimulation of mitogen-activated protein kinases mediated by cell type-dependent transactivation of receptor tyrosine kinases, J. Neurochem. 93 (2005) 899–909.
[14] A.S. Woods, F. Ciruela, K. Fuxe, L.F. Agnati, C. Lluis, R. Franco, S. Ferre, Role of electrostatic interaction in receptor–receptor heteromerization, J. Mol. Neurosci. 26 (2005) 125–132.
[15] S. Ferre, R. Baler, M. Bouvier, M.G. Caron, L.A. Devi, T. Durroux, K. Fuxe, S.R. George, J.A. Javitch, M.J. Lohse, K. Mackie, G. Milligan, K.D. Pfleger, J.P. Pin, N.D. Volkow, M. Waldhoer, A.S. Woods, R. Franco, Building a new conceptual framework for receptor heteromers, Nat. Chem. Biol. 5 (2009) 131–134.
[16] Y. Han, I.S. Moreira, E. Urizar, H. Weinstein, J.A. Javitch, Allosteric communication between protomers of dopamine class A GPCR dimers modulates activation, Nat. Chem. Biol. 5 (2009) 688–695.